RESEARCH ARTICLE

A novel process driving Alzheimer's disease validated in a mouse model: Therapeutic potential

Susan A. Greenfield[1] | Gregory M. Cole[2] | Clive W. Coen[3] | Sally Frautschy[2] | Ram P. Singh[2] | Marisa Mekkittikul[2] | Sara Garcia-Ratés[1] | Paul Morrill[1] | Owen Hollings[1] | Matt Passmore[1] | Sibah Hasan[1] | Nikisha Carty[4] | Silvia Bison[5] | Laura Piccoli[5] | Renzo Carletti[5] | Stephano Tacconi[5] | Anna Chalidou[5] | Matthew Pedercini[5] | Tim Kroecher[4] | Hubert Astner[5] | Philip A. Gerrard[5]

[1]Culham Science Centre, Neuro-Bio Ltd, Abingdon, UK

[2]Department of Neurology & Medicine, USA and Veterans Affairs Healthcare System, David Geffen School of Medicine at UCLA, Los Angeles, USA

[3]Faculty of Life Sciences & Medicine, King's College London, London, UK

[4]Manfred Eigen Campus, Evotec SE, Hamburg, Germany

[5]Aptuit, Evotec (Verona) Srl, Verona, Italy

Correspondence
Susan A. Greenfield, Neuro-Bio Ltd, Building F5, Culham Science Centre, Abingdon, OX14 3DB, UK.
Email: susan.greenfield@neuro-bio.com

Abstract

Introduction: The neuronal mechanism driving Alzheimer's disease (AD) is incompletely understood.

Methods: Immunohistochemistry, pharmacology, biochemistry, and behavioral testing are employed in two pathological contexts—AD and a transgenic mouse model—to investigate T14, a 14mer peptide, as a key signaling molecule in the neuropathology.

Results: T14 increases in AD brains as the disease progresses and is conspicuous in 5XFAD mice, where its immunoreactivity corresponds to that seen in AD: neurons immunoreactive for T14 in proximity to T14-immunoreactive plaques. NBP14 is a cyclized version of T14, which dose-dependently displaces binding of its linear counterpart to alpha-7 nicotinic receptors in AD brains. In 5XFAD mice, intranasal NBP14 for 14 weeks decreases brain amyloid and restores novel object recognition to that in wild-types.

Discussion: These findings indicate that the T14 system, for which the signaling pathway is described here, contributes to the neuropathological process and that NBP14 warrants consideration for its therapeutic potential.

KEYWORDS
5XFAD, acetylcholinesterase, alphaLISA, Alzheimer's disease, amyloid beta, basal forebrain, Braak stage, cortex, hippocampus, NBP14, novel object recognition, T14

1 | BACKGROUND

The basic mechanism driving Alzheimer's disease (AD), as well as Parkinson disease and motor neuron disease, may be the deleterious activation in the maturity of a signaling system that had been beneficial in development.[1–4] Toxic effects may occur if this system is activated in the mature brain in response to a blow to the head,[5] ischemia,[6] or a decline in scavenging mechanisms.[7] Such a phenomenon would exemplify antagonistic pleiotropy, as proposed in George Williams' evolutionary explanation of senescence.[8,9] His theory concerns tradeoffs

between early life benefits and late-life detriments and is consistent with a decline in the potency of natural selection with age. The signaling molecule driving this particular trophic-toxic process is posited to be T14,[1,2] a 14mer peptide that binds to an allosteric site on alpha-7 nicotinic receptors.[10,11] This peptide derives from the C-terminus of acetylcholinesterase (AChE),[12] a protein that has long been implicated in AD.[13] Inhibiting the hydrolyzing action of AChE on acetylcholine (ACh), with drugs such as galantamine, increases the availability of synaptic ACh; such treatments are clinically useful in AD, a finding that validates the cholinergic hypothesis for this disease.[13] Enhancing ACh availability may also favor the cholinergic alleviation of inflammation,[14] a hallmark of AD.[15] Conversely, transgenic mice overexpressing AChE show AD-like cognitive impairment[16]; the authors of that study speculated that the excess AChE "may have effects that relate to the potential noncatalytic function(s) of this intriguing protein." We now hypothesize that T14, a peptide cleaved from AChE,[12] drives such effects.[1] This peptide, which shares a partial sequence homology with amyloid,[1,2] has been shown to promote amyloid beta production and tau phosphorylation, thereby replicating the principal features of AD pathology.[17] It also enhances calcium influx,[10] modulates plasticity (ie, long-term potentiation [LTP]),[8] acts as a developmental signaling molecule,[2] and is bioactive in a range of tissues including rat hippocampal organotypic cultures[2] and ex vivo brain slices from hippocampus[10] or the rat prefrontal cortex.[18]

In the normal adult brain, there is a prevalence of G4, the tetramer that constitutes membrane-bound AChE, over G1, the monomeric form of AChE.[19] The latter is the parent molecule for T14.[12] In contrast, in the early embryonic human brain, G1 exceeds G4.[19] the prevalence of G1 is consistent with an involvement of its cleavage product in development.[1] Notably, it also exceeds G4 in various brain regions in AD.[19] Thus, the initially beneficial developmental effects of T14[10] may turn excitotoxic with aging, when tolerance to calcium influx is lower,[20] via an allosteric site on alpha-7 nicotinic receptors.[10] The capacity of the peptide to upregulate that receptor's messenger RNA (mRNA) and protein expression and to enhance its trafficking to the plasma membrane[11] may promote a vicious cycle. Hence, the process that drives the pathology may be an aberrant recapitulation of T14's developmental actions.[1]

The present study was designed to characterize the T14 system in two pathological contexts—AD and the 5XFAD (Five Times Familial AD Mutations) mouse model of AD—and to explore whether a T14 antagonist has therapeutic potential. For the immunohistochemical studies on human and mouse brains, a polyclonal antibody was used; it was raised against the T14 C-terminus and does not cross-react with AChE or amyloid.[17] T14 immunoreactivity in the hippocampus, a region severely afflicted by the disease, was assessed in early versus late-stage AD and in 5XFAD mice compared with their FAD-negative counterparts, F1 offspring of the same background strain lacking the transgene.[21] 5XFAD mice provide a valid, rapid-onset, aggressive amyloid model displaying neuropathological and neuropsychological AD-like hallmarks.[21] The age-dependent development of cognitive deficits in these animals is comparable to that in AD; the earliest observable impairment is in spatial working memory followed by

HIGHLIGHTS

- The T14 peptide system is characterized in Alzheimer's disease (AD) and the 5XFAD transgenic model
- AD and 5XFAD mice show T14 immunoreactivity in neurons and adjacent plaques
- NBP14, a cyclized version of T14, dose-dependently displaces T14 in AD
- Intranasal NBP14 treatment for 14 days reduces amyloid in 5XFAD mice
- The NBP14 treatment protects the 5XFAD mice from impaired novel object recognition

RESEARCH IN CONTEXT

1. **Systematic Review**: Over the past 50 years, evidence has accumulated within the literature, and from our own research, that acetylcholinesterase has additional, non-catalytic roles. Diverse findings demonstrate its role as a signaling molecule, irrespective of cholinergic transmission. The beneficial, trophic actions of this system during development may turn excitotoxic in maturity and consequently drive Alzheimer's disease (AD). Twenty years ago, a 14mer peptide cleaved from the C-terminus, T14, was identified as the salient agent.

2. **Interpretation**: Our findings on T14 localization and levels are comparable in AD brains and in the 5XFAD transgenic mouse model. NBP14, a cyclized antagonist of T14, displaces T14 from alpha-7 nicotinic receptors in the AD hippocampus. In 5XFAD mice, it lowers brain amyloid and protects memory.

3. **Future Directions**: Further research will pursue the novel idea that T14 is the key signaling molecule driving AD and assess the potential of NBP14 as a therapeutic.

deficits in recognition memory.[22,23] Female 5XFAD mice were used in the present study because they display more severe amyloid pathology than 5XFAD males[21,24–26]; within the hippocampal formation, the females show a consistently higher density of amyloid plaques than age-matched male mice.[24]

NBP14 is a cyclic form of the linear T14 peptide, acting as an antagonist.[17] It binds at alpha-7 receptors some 50 times more effectively than galantamine,[17] which recognizes not only the allosteric alpha-7 site[27] but also, unlike NBP14, modulates the closely related $\alpha 4\beta 2$ nAChR,[27] a receptor not activated by T14.[17] Irrespective of the functional efficacy of NBP14 in vitro ,[3,17,28] including its capacity to displace T14-binding in post-mortem AD brains as assessed here, its therapeutic potential requires access to the brain in vivo. Intranasal

administration has been found to be more effective than intravenous or oral routes for peptides to cross the blood-brain barrier.[29] To evaluate the effectiveness of such treatment, 5XFAD mice were given intranasal vehicle or NBP14 (10 mg/kg, 10 μL/mouse) twice weekly for up to 14 weeks. Its penetration into the brain and its effects on memory and brain amyloid were assessed. The treatment started at 7- to 10 weeks of age, sufficiently early to allow the drug to interact with its targets before the neuropathological processes commenced.[21]

Cognitive performance was evaluated with the Novel Object Recognition Test (NORT), a non-spatial, non-aversive memory test widely used in assessing drug effects on recognition memory.[30] The NORT is based on the innate preference of animals to explore a novel over a familiar object, requiring memory of the object presented in the previous trial. The 5XFAD mice were monitored in the NORT prior to the initial intranasal vehicle or NBP14, followed by further testing after 6 and 14 weeks. Naive wild-type mice not subjected to the treatment were included in the study and tested in the NORT in parallel with 5XFAD mice.

Brain amyloid immunoreactivity was investigated in satellite 5XFAD mice after vehicle or NBP14 treatment for 6 weeks and at the terminal time point of 14 weeks in the 5XFAD mice studied in the NORT. The cortex, hippocampus, and basal forebrain were analyzed, being key sites affected with extensive amyloid deposits in AD.[31]

2 | MATERIALS AND METHODS

2.1 | Human and mouse brains

Human hippocampal blocks were provided by Dr Wayne Poon (UCI MIND Tissue Repository Gillespie Neuroscience Research Facility at University of California, Irvine) and the National Brain Bank (https://neurobiobank.nih.gov/about/) from all Braak stages, male and female, with post-mortem interval (PMI), apolipoprotein E (*APOE*) gene, plaque stage, and clinical syndrome described. The human hippocampus samples analyzed in western blots for T14 were provided by the Oxford Brain Bank, and classified as Braak stages 0, I, II, V, or VI. The mice used for amyloid immunohistochemistry and the parallel behavioral study were wild-type (WT) B6SJL female (*n* = 15) and transgenic 5XFAD female (*n* = 95), supplied by Jackson Laboratories (Bar-Harbor, ME, USA). The mice were 4- to 8-weeks-old at the time of arrival (maintained *n* = 5/cage, 12-hour light/dark cycle, lights from 6:00 hours, 20°C–22°C). Female mice were studied because the amyloid pathology in 5XFAD transgenics is more severe in female than male mice.[21,24–26] The 5XFAD mice used for T14 immunohistochemistry were purchased from JAX Genomic Medicine (Farmington, CT, USA); they were 34- to 40-weeks-old when studied. Experimental procedures were conducted between 9:00 and 16:00 hours and undertaken under authorization from the Italian Ministry of Health (Project Internal Code n. 820/2019-PR), in accordance with Italian Legislative Decree No. 26/2014, or from the Institutional Animal Care Use Committee USA (VA IACUC #08032-09); ARRIVE Guidelines were followed for reporting in vivo experiments (see Supplementary Materials).

2.2 | Western blot detection of T14

Western blots were carried out as described previously.[17] Briefly, ≈0.2 g of frozen human brain tissue was thawed and homogenized in ice-cold Neuronal Protein Extraction Reagent supplemented with phosphatase and protease inhibitors. Buffer , 1 mL, was added per 0.2 g of brain tissue. Homogenate was centrifuged (16,000 × g, 30 minutes, 4°C) and supernatant quantified for protein. One hundred micrograms of protein was mixed with 4× Laemmli sample buffer (62.5 mM Tris-HCl pH 6.8, 10% glycerol, 1% LDS, 0.005% Bromophenol Blue, 50 mM dithiothreitol [DTT]), heated to 50°C (10 minutes), and loaded onto 4%–20% Mini-PROTEAN TGX Precast Protein Gels, 10-well, 50 μL. Proteins were separated by electrophoresis, transferred to PVDF (0.45 μm) membrane, and blocked (1 hour; RT) with 5% Blotting Grade Blocker Non-Fat Milk in Tris-buffered saline plus 0.05% Tween 20 (TBS-T 0.05%). The membrane was incubated overnight with T14 antibody (stock 1 mg/mL, dilution 1:1000) as described previously.[17] Membranes were washed, incubated with secondary antibody (1:10000), washed, and immunoreactivity visualized as described previously. Bands were quantified using ImageJ, and unpaired *t* tests were performed using GraphPad Prism9.0.

2.3 | AlphaLISA detection of T14-alpha-7 complex

Samples were extracted from homogenized human brain tissue using PerkinElmer lysis buffer and the protein concentration determined using the BCA method. For 100 mg tissue homogenization, 1 mL of lysis buffer was used. Five cycles of 40 second pulse, and 10 second breaks, on a shielded homogenizer were used for each sample. Samples were centrifuged at 40°C, 15000 rpm (15 minutes) for supernatants; these were diluted in PerkinElmer Assay buffer and used to measure T14-alpha-7 nicotinic receptor complexes in the presence of NBP14 (concentrations 0.065μM -900μM) with AlphaLISA following the manufacturer's protocol.[32] The antibodies were biotinylated BTX on SA-donor beads and anti-rabbit T14 on acceptor beads; results read in an AlphaLISA Reader.

2.4 | Immunohistochemistry

Details for the immunohistochemical processing of human and mouse brain tissue and image analysis are provided under Supplementary Materials.

2.5 | NBP14 synthesis and stability

NBP14 was synthesized by Genosphere Biotechnologies (Paris, France) as described previously.[17] Confirmation of its stability at RT is described under Supplementary Materials.

2.6 | Intranasal (IN) dosing with NBP14

The NBP14 dose was freshly dissolved in vehicle (0.9% NaCl) to obtain the required concentrations at a final volume of 10 μL for the corresponding dose of 10 mg/kg for each animal. Animals were sedated with isoflurane. The IN dose was administered at 5 μL per nares using a pipette allowing the animals to sniff the drops into the nasal cavity over the following 10 minutes.

2.7 | Blood-brain exposure to NBP14

A preliminary pharmacokinetic (PK) study of acute intranasal (IN) administration of NBP14 at 30 mg/kg was carried out with brains collected at 0.25, 0.5, 2, and 8 hours post NBP14 administration. The PK profile of NBP14 (10 mg/kg; IN) following repeated administration was assessed in 5XFAD mice at four time points (as described in Figure 2). Thirty minutes after treatment administration, following an overdose of isoflurane, blood samples from the descending vena cava and the brain were collected. The group of mice sampled 2 days after the final treatment in week 14 were not treated with NBP14 on the day of blood and brain tissue collection to test for any accumulation of the drug.

Blood and brain samples were processed immediately after animal sacrifice by dilution or homogenization followed by protein precipitation with three volumes of acetonitrile containing 0.1 ng/mL of leucine encephalin. After centrifugation, supernatant was diluted with 1.5 volumes of H_2O. The samples were assayed by LC-MS/MS analysis with an optimized analytical method on an Acquity HSS T3 column 1.7 μm 50 × 2.1 mm (Waters, Milford MA, USA). A binary chromatographic gradient of Phase A (water +0.1% formic acid) and Phase B (acetonitril +0.1% formic acid) was used for separation at a flow rate of 0.65 mL/minute. Quantitation was performed in multiple reaction monitoring on an API 6500+ Instrument (Sciex, Framingham, MA USA) NBP14 (m/z 462.3 → 110.1) and leucine enkephalin (m/z 556.0 → 397.0).

2.8 | NORT

The cognitive performance of mice was tested using the NORT. Object exploration was defined as active interaction with the object, that is, sniffing or touching the object with the nose and/or forepaws. In contrast, circling, sitting on, or leaning close to the object were not considered active exploration. The results were expressed as total time (seconds) spent by animals exploring the object. A recognition index calculated for each animal was the percentage of time spent exploring the familiar versus the novel object. A criterion of minimal object exploration was used to exclude animals with naturally low levels of spontaneous exploration: the two animals that explored for < 10 seconds during both the acquisition and choice sessions were not included in the study. General activity was also recorded as the total time spent in locomotor activity, rearing, and self-grooming behaviors. 5XFAD mice were

tested in the NORT at three time points, and brains were then removed and processed as described above.

2.9 | Statistical analysis

Statistical analyses were conducted using either GraphPad Prism7.0 (GraphPad Software) or SAS 9.4. NORT data were analyzed by one-way analysis of variance (ANOVA) for each treatment group at each time point, and in other cases such as general activity and recognition index, a two-way ANOVA followed by Bonferroni's post hoc test was used. A repeated-measures (treatment × time) approach was used for body weight, with baseline values at week 0 included as a covariate in the analysis (analysis of covariance [ANCOVA]), followed by Fisher's Least Significance Difference (LSD) post hoc test. Histological data were analyzed using the unpaired Student's t-test.

3 | RESULTS

3.1 | T14 in the post-mortem Ad brain and transgenic mouse model

Western blots of the AD hippocampus showed a single T14-reactive band that increased ≈2-fold from early (Braak 0-II) to late stages (Braak V-VI; Figure 1A, C). This signal could be eliminated by immunoneutralization or omission of the primary antibody. The binding of T14 to the alpha-7 receptor was investigated with AlphaLISA.[32] This approach revealed a greater level of T14-binding in late-stage AD (Braak V-VI) compared with Braak I-II (Figure 1B). Immunohistochemistry of hippocampal sections from late-stage AD showed T14-immunoreactive neurons in the immediate vicinity of T14-immunoreactive plaques (Figure 1D); the advanced state of the disease is confirmed by immunohistochemistry for phosphorylated Tau in adjacent sections (Figure 1E).

In the hippocampus of 5XFAD mice, T14 immunoreactivity was at a particularly high incidence in the subiculum (Figure 1F). Neurons immunoreactive for T14 were seen in the immediate vicinity of T14-immunoreactive plaques (Figure 1H, J). The immunoreactive signal for T14 was lost following neutralization of the primary antibody with the peptide (Figure 1G, I, K). In FAD-negative mice, the hippocampus contained only a light degree of T14 immunoreactivity; there were no T14-immunoreactive plaques (Figure 1L).

3.2 | Antagonizing T14 with a cyclized variant: NBP14

The capacity of NBP14 to displace T14-binding to the alpha-7 receptor in the human hippocampus in late-stage AD brains was investigated with AlphaLISA; this revealed a clear dose-response (Figure 1M), with an IC_{50} of 61.4 μM.

To assess the penetration of NBP14, blood and brain tissue were collected at four time points: following the initial treatment, after 6 and 14 weeks of twice-weekly dosing, and, to test for any

Human Hippocampus

Mouse Hippocampus
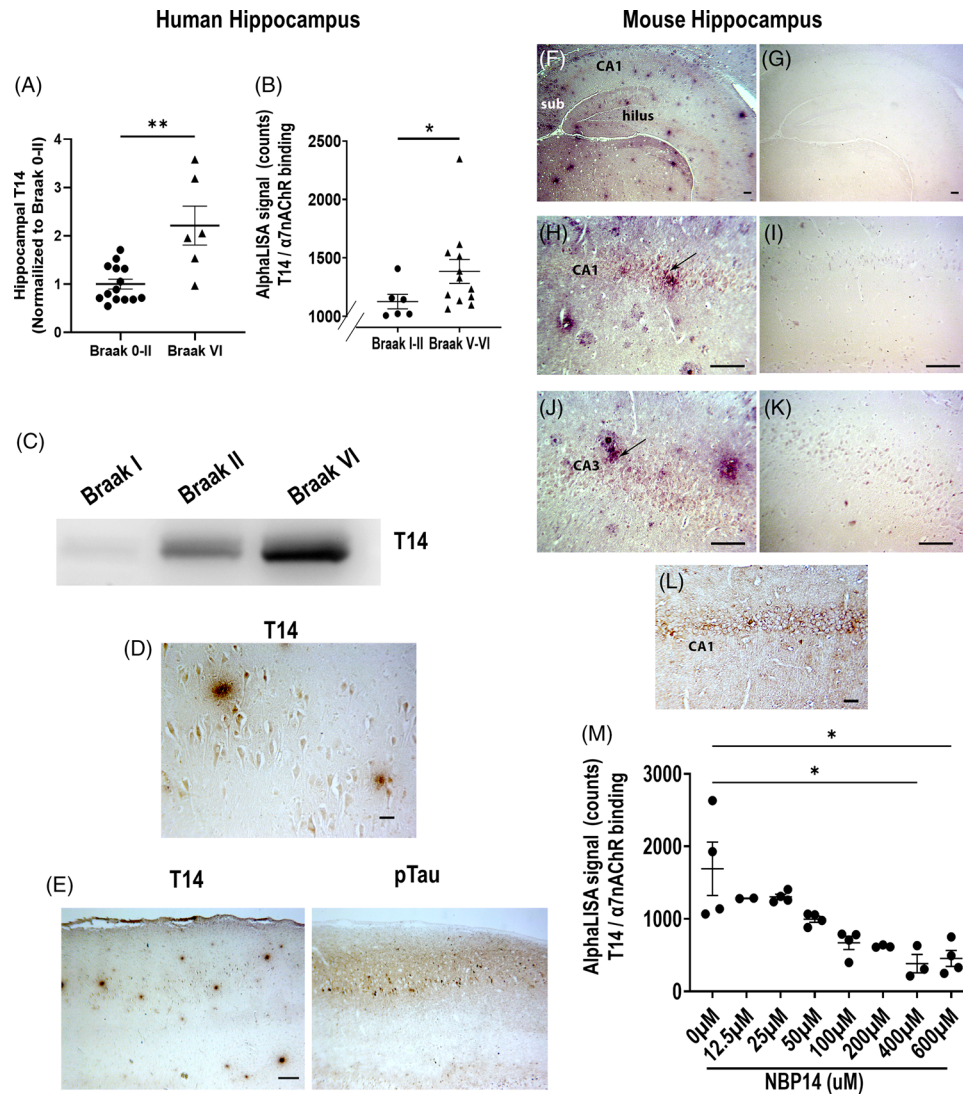
FIGURE 1 (A) Quantification of hippocampal T14 (mean $\pm$ SEM) normalized to the data for Braak 0-II ($n = 14$), showing a significant increase at Braak VI ($n = 6$, Mann-Whitney test). (B) T14-alpha-7 receptor binding using AlphaLISA in early stage (Braak I-II, $n = 6$) and late stage (Braak V-VI, $n = 12$, Mann-Whitney test) hippocampal tissue. (C) Examples of western blots for hippocampal T14 at Braak I, II, and VI, showing an increase at the later stage. (D, E) T14- and p-tau-immunoreactivity in Alzheimer's disease; representative photomicrographs of the CA1 region of the hippocampus in an 85-year-old man, Braak VI. (D) T14-immunoreactive neurons in proximity to T14-immunoreactive plaques. (E) T14- and p-tau-immunoreactivity in adjacent sections. (F, H, J) Representative photomicrographs of hippocampal T14-immunoreactivity in the 5XFAD mouse; (G, I, K) adjacent coronal sections showing loss of T14-immunoreactivity following immunoneutralization of the primary antibody. (L) The Cornu ammonis 1 (CA1) region of the hippocampus in an FAD-negative mouse, showing light T14-immunoreactivity in pyramidal neurons and no T14-immunoreactive plaques. (M) Dose-dependent effects of NBP14 in displacing T14-alpha-7 binding in advanced AD (Braak III-VI, $n = 3$-4, two-way ANOVA) hippocampal tissue (NBP-14 IC50 = 61.4 μM); data are mean $\pm$ SEM. *$P < .05$, ** $P < .01$. Scale bars: 70 μm (D), 210 μm (E), 140 μm (F, G, L), 40 μm (H-K), sub, subiculum (F). Arrows (H, J), examples of a T14-immunoreactive neuron adjacent to a T14-immunoreactive plaque

accumulation of the drug, 2 days after the final treatment in Week 14. The concentrations of NBP14 in blood and brain and their ratios are shown (Figure 2A-C). An absence of compound accumulation was indicated by the satellite group assessed 2 days after the final treatment in Week 14 (data not shown).

Body weight was measured in the transgenic mice treated twice weekly with vehicle (5XFAD-VEH) or NBP14 (5XFAD-NBP14) over 14 weeks (Figure 2D).

3.3 | Effects of chronic intranasal NBP14 on memory in AD mouse model

There were no significant differences across the three groups—untreated wild-types, 5XFAD-VEH, and 5XFAD-NBP14—at any time point for general activity, recorded as the time spent in locomotion, rearing, and self-grooming, indicating no non-specific effects of NBP14 on arousal levels (Figure 2E).
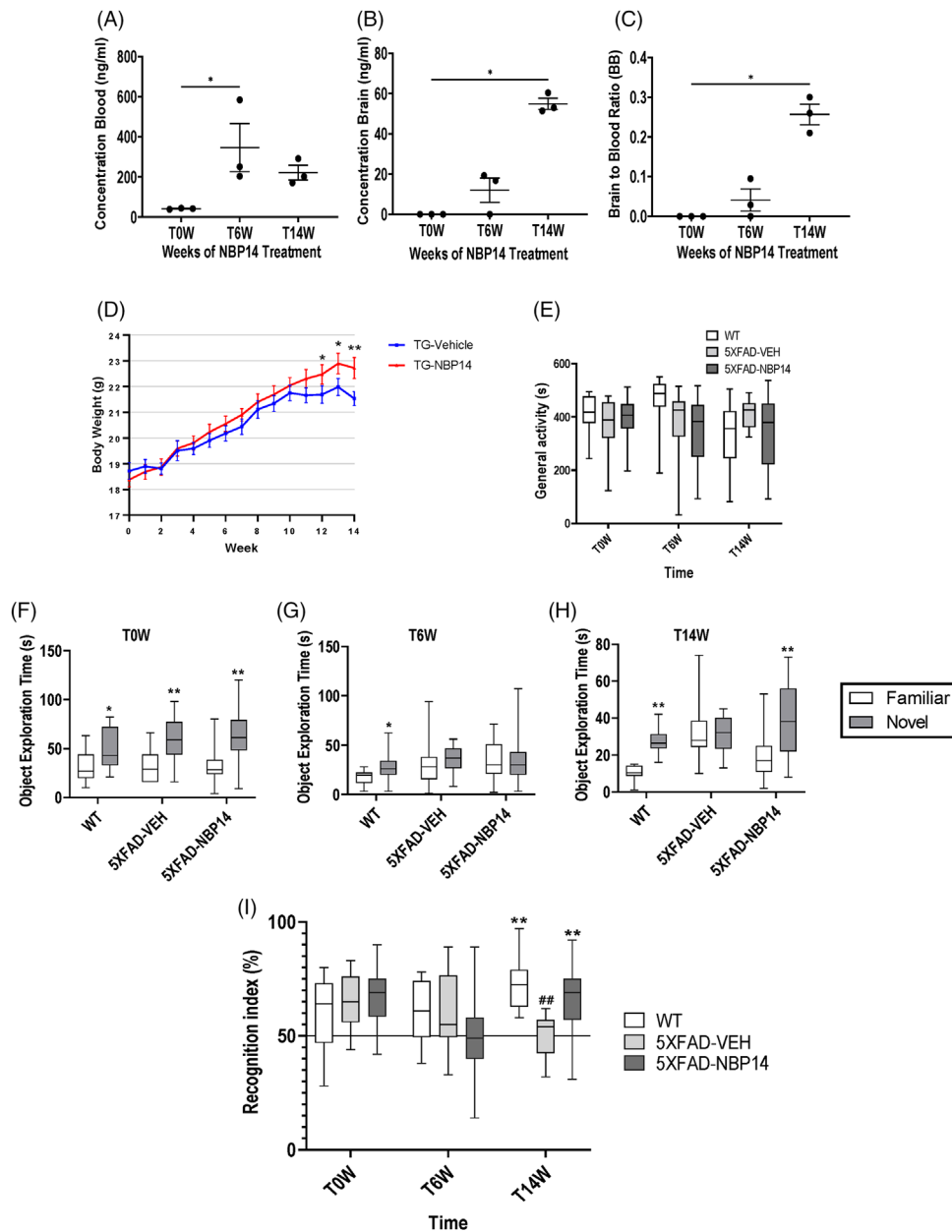
FIGURE 2 (A-C) Blood and brain concentrations of NBP14 in 5XFAD mice following intranasal treatments with NBP14 (10 mg/kg) and brain-to-blood ratio. The samples ($n = 3$ for each time point) were collected 30 minutes after a single initial treatment in T0W and after twice weekly treatments for 6 weeks or 14 weeks; additional samples were collected 2 days after the final treatment in T14W, to test for any accumulation of the drug. Friedman multiple comparison tests showed differences in NBP14 concentrations in blood between T0W and T6W ($P = .0286$) but not T0W and T14W, and in the brain between T0W and T14W ($P = .0495$) but not T0W and T6W; the blood-to-brain ratio increased significantly by T14W ($P = .0306$) but not by T6W. (D) Body weight (mean of biweekly measurements) of 5XFAD mice (5XFAD-VEH and 5XFAD-NBP14) over the 14-week treatment period. Weights taken immediately before (Day 0) and following vehicle or NBP14 treatment twice weekly for 14 weeks ($n = 14$–28). Analysis of covariance revealed no overall effect of treatment per se ($F(1, 39) = 2.17, P = .1484$), but an effect of time ($F(13, 520) = 90.22, P < .0001$) and a difference for the main effect of treatment x time ($F(13, 520) = 1.90, P = .0281$). Pairwise comparison showed a significant difference between the 5XFAD-VEH and 5XFAD-NBP14 mice at 12 to 14 weeks of treatment. (E-H) Novel Object Recognition Test performance in wild-type (WT) and 5XFAD mice. (E) Time (s = seconds) spent in general activity by untreated WT and 5XFAD mice prior to and after 6 and 14 weeks of vehicle or NBP14 treatment ($n = 13$-28; one-way ANOVA showed no significant differences> $P > .05$). (F-H) Total object exploration time (s = seconds) for familiar and novel objects in 5XFAD mice: (F) before treatment (T0W) and (G) after 6 weeks (T6W) or (H) 14 weeks (T14W) of intranasal vehicle or NBP14 (10 mg/kg); untreated age-matched WT were tested concurrently ($n = 13$ for vehicle, 28 for NBP14 one-way ANOVA). (I) Recognition Index showing percentage of recognition above chance (50%) levels, calculated as time spent exploring the novel object/time exploring novel + familiar object in untreated WT and 5XFAD mice prior to and at 6 and 14 weeks of vehicle or NBP14 treatment ($n = 13$–28); data are mean ± SEM. * $P < .05$, ** $P < .01$ versus 5XFAD-VEH; ## $P < .01$ versus baseline value (T0W) of the group in question, two-way ANOVA followed by Bonferroni's post hoc). T0W, Week 0; T6W, Week 6; T14W, Week 14.

At the times of behavioral testing—Week 0, Week 6, and Week 14— the estimated age of the 5XFAD and wild-type mice was 7–10 weeks, 13–16 weeks and 21–24 weeks. Assessment before the start of the treatment showed that the three groups discriminated between the novel and familiar object after a 1-hour retention interval, spending a significantly longer time exploring the novel object (Figure 2F).

At Week 6 (13–16 weeks of age), impaired performance was observed in 5XFAD-VEH and 5XFAD-NBP14 mice (Figure 2H). At Week 14, there was continued discrimination in wild-types (Figure 2I) and continued failure to discriminate in 5XFAD-VEH mice (Figure 2H). However, 5XFAD-NBP14 mice showed a significant increase in time spent exploring the novel versus the familiar object (Figure 2H), an effect consistent with a reversal of cognitive impairment. The NBP14 treatment significantly increased the Recognition Index in 5XFAD mice (Figure 2I). Two-way ANOVA showed an effect of time and a considerable difference for the main effect of treatment x time. Bonferroni's post hoc test showed that the Recognition Index was significantly higher in 5XFAD-NBP14 mice than in the 5XFAD-VEH mice ($P < .01$) and did not differ significantly different from that of the wild-type mice (Figure 2I).

3.4 | Effects of chronic intranasal NBP14 on brain amyloid in AD mouse model

In 5XFAD mice after 6 weeks of vehicle treatment, intracellular amyloid beta (Aβ) immunoreactivity was observed throughout the frontal cortex and hippocampal formation, particularly in the subiculum, with only a low incidence in the basal forebrain (Figure 3A, 3B and 3C). At this time, the 5XFAD-NBP14 mice showed a significantly lower incidence of intracellular Aβ immunoreactivity than the 5XFAD-VEH mice, by 53% in the hippocampus (Figure 3A) and 38% in the frontal cortex (Figure 3B), but there was no appreciable effect of NBP14 on the minimal amount of intracellular Aβ in the basal forebrain region (Figure 3C). Further accumulation had occurred by the time the mice were 21–24 weeks old, after 14 weeks of vehicle treatment (Figure 3D and 3E), by which time plaques had become apparent in the basal forebrain (Figure 3F). The 5XFAD-NBP14 group, in comparison with the 5XFAD-VEH group, showed a significant reduction in extracellular Aβ by 50% in the hippocampus (Figure 3D), 38% in the frontal cortex (Figure 3E), and 42% in the basal forebrain (Figure 3F).

4 | DISCUSSION

The presence of T14-immunoreactive neurons in proximity to T14-containing plaques in the hippocampus in humans with late-stage AD and in 5XFAD mice is consistent with the model presented (Figure 4) for the role of T14 in the neuropathological process. A comparable distribution has been reported for Aβ-immunoreactive neurons and plaques in the 5XFAD hippocampus by Oakley et al.[21] Furthermore, T14 immunoreactivity is at a particularly high incidence in the subiculum, as reported previously for Aβ immunoreactivity in this model.[21]

These findings, obtained in human and mouse brains, indicate that T14 is prominent in late-stage AD and in 5XFAD mice. Hence, intercepting the binding of T14 to alpha-7 receptors could be a strategy for combating AD. Approaches focusing on this receptor as a therapeutic target in AD are not new; however, candidate antagonists to date have met with only limited success,[17] perhaps because this site in AD is already occupied by endogenous T14, acting as a more effective ligand than the exogenous compounds.

The results of the present study demonstrate penetration into the brain, increasing by ≈6-fold between Week 6 and Week 14 of treatment. In contrast, the circulating level of the antagonist remained unchanged between these time points, albeit at a far higher level than after the first treatment in Week 0. The increase in the concentration of NBP14 in the brain, relative to blood, by Week 14 may reflect a gradual change in the permeability of the blood brain barrier as reported for AD.[33,34]

The effect of chronic NBP14 treatment on body weight in the 5XFAD mice indicates a beneficial action sufficient to offset the slower weight gain typically seen in these animals.[22,35] Previous research found that their cognitive performance starts to decline between 12 and 24 weeks of age[23]; this is consistent with the unimpaired discrimination between novel and familiar objects at 7–10 weeks of age prior to the onset of treatment in the present study.

Although the cognitive performance of the 5XFAD mice was improved by NBP14 only after 14 weeks of treatment (ie, 21–24 weeks of age), a decrease in intracellular amyloid was observed as early as 6 weeks after starting the treatment. This apparent delay in the behavioral effects may relate to the greater amount of NBP14 reaching the brain by Week 14 of treatment and/or the greater amount of neuronal change required for this functional effect to be realized. Intraneuronal Aβ accumulates in the 5XFAD brain from 6 weeks of age, before plaques form.[21] By Week 14 of vehicle treatment, the amyloid immunoreactivity was most readily observed as extracellular plaques; in the NBP14-treated 5XFAD mice, this plaque-related Aβ immunoreactivity was reduced markedly in key brain areas linked to AD: hippocampus, frontal cortex, and basal forebrain. Given the evidence that intraneuronal aggregates of Aβ play a significant role in neurodegeneration and amyloid plaque formation,[36] the effect of NBP14 in reducing amyloid could result from its blockade of an intracellular cascade initiated by T14 at alpha-7 receptors.[2] The proposed mechanisms of action of T14 and NBP14 are presented in Figure 4.

T14 is a signaling molecule that putatively drives neurodegeneration. The present study shows that hippocampal T14 increases with the progression of AD and is a conspicuous feature of the 5XFAD mouse model. NBP14, a cyclic version of T14, has the capacity to displace T14-binding at alpha-7 receptors.[3,17,28] NBP14 has been shown previously to block the various effects of T14 in vitro [17] and ex vivo .[3,28] The current findings demonstrate the capacity of this drug to displace T14-binding in post-mortem AD brains and to access the mouse brain in vivo by the intranasal route. In summary, NBP14 has protective actions in an established animal model of AD, evidenced by cognitive performance, neurochemistry, and body-weight gain. The present findings suggest
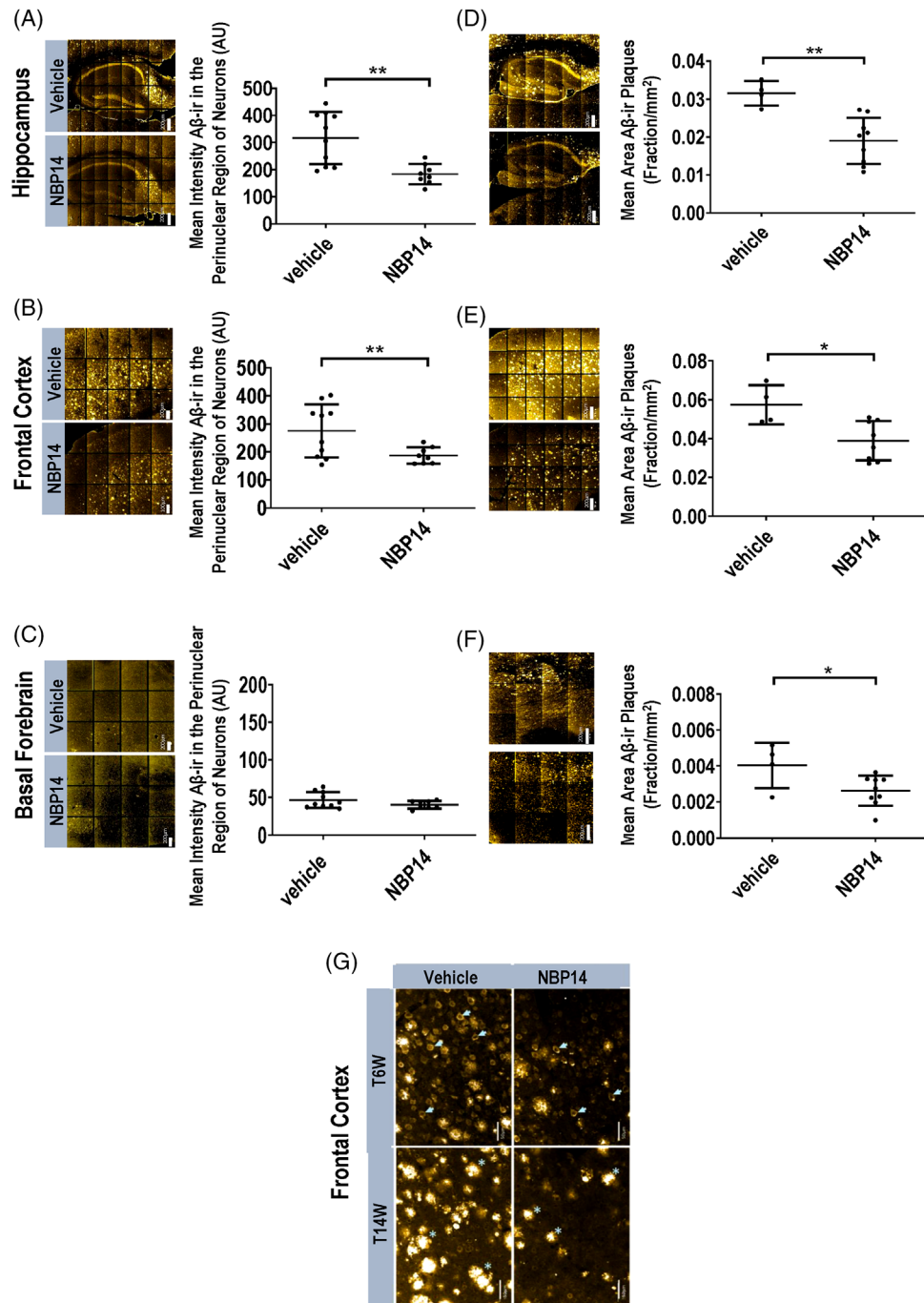
FIGURE 3 Immunohistochemistry for Aβ (gold) in sagittal sections from 5XFAD mice following intranasal treatment with vehicle (saline) or NBP14 (10 mg/kg) for (A, B, C) 6 weeks or (D, E, F) 14 weeks; scale bars: hippocampus 6/14 weeks (w) = 200 μm; frontal cortex 6w = 100 μm, 14w = 200 μm; basal forebrain 6/14w = 200 μm. Aβ deposits were detected in the hippocampus and frontal cortex in both groups at both time points; in contrast, Aβ was detected in the basal forebrain only in the groups that had been treated for 14 weeks, at which time the animals were 21- to 24-weeks-old. Levels of intracellular Aβ were calculated in the groups receiving treatment for 6 weeks as the mean intensity in the perinuclear region (AU, arbitrary units), and in the groups receiving treatment for 14 weeks extracellular Aβ was calculated as the mean area of immunoreactivity. (G) Higher magnification examples showing intracellular amyloid and extracellular plaques in frontal cortex after, respectively, 6 and 14 weeks of vehicle or NBP14. Arrows show examples of intraneuronal Aβ; asterisks show examples of extracellular Aβ plaques; scale bars = 50 μm. At 6 weeks of treatment (A, B, C) n = 10 for vehicle, n = 8 for NBP14; at 14 weeks of treatment (D, E, F) (n = 4 for vehicle, n = 8 for NBP14. Data are mean ± SEM. * P < .05; **P < .01, unpaired t-tests)

(A) Cascade 1

(B) Cascade 2

(C) Cascade 3
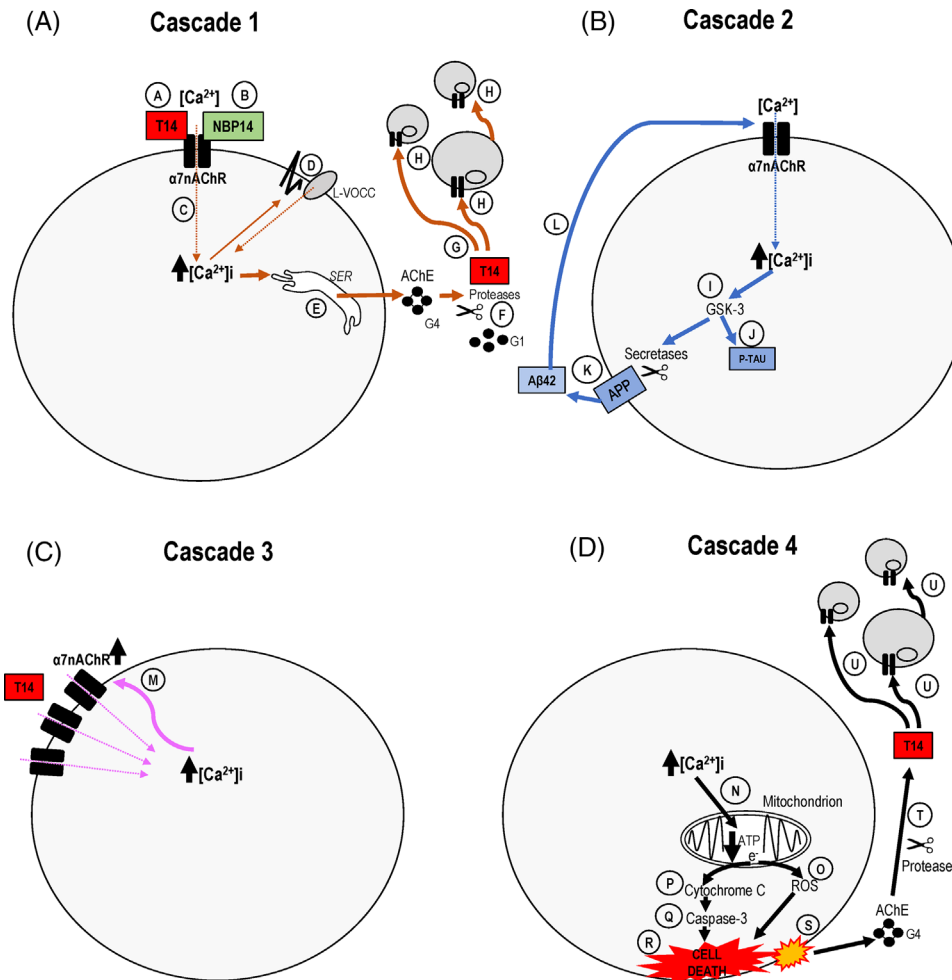
(D) Cascade 4

FIGURE 4 The T14 system participates in at least four interactive cascades. Cascade 1 (brown): (A) T14 binds at its allosteric site on the alpha-7 receptor[10] unless (B) this is blocked by NBP14.[3,17,28] (C) T14 binding increases calcium influx (dotted line),[17] causing (D) depolarization and activation of voltage sensitive calcium channels (L-VOCC).[17] (E) Elevated calcium triggers AChE release (G4 tetramer) from intracellular storage, for example, smooth endoplasmic reticulum (SER)[37] into extracellular space.[1] Subsequently (F) proteases, for example, Insulin Degrading Enzyme, cleave T14 from the parent molecule,[38] leaving the G1 monomer without the T14-containing disulfide bonds and therefore unable to oligomerize.[39] (G) T14 diffuses to act (H) on alpha-7 receptors on neighboring cells, thereby perpetuating the cycle. Cascade 2 (blue): (I) The T14-induced increase in intracellular calcium activates the enzyme GSK-3[17] resulting in (J) tau phosphorylation[17] and (K) cleavage of amyloid beta from membrane bound APP by secretases,[40] resulting (L) in enhanced calcium toxicity via alpha-7 receptors.[17] (c) Cascade 3 (pink): (M) The T14-induced increase in intracellular calcium causes upregulation of its target alpha-7 receptors and their trafficking to the plasma membrane,[11] further facilitating T14 effects. (d) Cascade 4 (black): The T14-induced increase in intracellular calcium leads to (N) calcium uptake into mitochondria, decreasing ATP synthesis accompanied by electron leakage, thereby (O) increasing free radical generation (ROS), (P) triggering cytochrome C release,[41] followed by (Q) caspase-3 activation and (R) cell death.[42] (S) Consequent membrane disintegration makes previously membrane-bound AChE (G4) vulnerable to protease degradation, leading (T) to increased T14 for diffusion to neighboring neurons (U) perpetuating the T14 process

that NBP14 and the T14 system merit further evaluation in elucidating the mechanism that drives AD.

CONFLICT OF INTEREST

Susan Greenfield is the founder and CEO of Neuro-Bio Limited and holds shares in the Company. She is the inventor in all Neuro-Bio patents. Neuro-Bio has a patent portfolio that currently includes 15

AUTHOR CONTRIBUTIONS

Conceptualization: Susan A. Greenfield. Methodology: Gregory M. Cole, Ram P. Singh, Sally Frautschy, Nikisha Carty, Silvia Bison, Laura Piccoli, Renzo Carletti, Stephano Tacconi, Anna Chalidou, Matthew Pedercini, Tim Kroecher, Hubert Astner. Investigation: Gregory M. Cole, Ram P. Singh, Sally Frautschy, Silvia Bison, Laura Piccoli, Renzo Carletti, Stephano Tacconi, Anna Chalidou, Matthew Pedercini, Tim Kroecher, Hubert Astner. Project administration: Susan A. Greenfield, Philip A. Gerrard. Supervision: Susan A. Greenfield, Philip A. Gerrard. Writing – original draft: Susan A. Greenfield, Clive W. Coen, Sara Garcia-Ratés, Paul Morrill. Writing – review & editing: Susan A. Greenfield, Clive W. Coen, Sara Garcia-Ratés, Paul Morrill.

ORCID

Susan A. Greenfield https://orcid.org/0000-0001-6730-5149
Gregory M. Cole https://orcid.org/0000-0002-6848-7455
Clive W. Coen https://orcid.org/0000-0003-1303-216X
Sally Frautschy https://orcid.org/0000-0003-0194-0363
Marisa Mekkittikul https://orcid.org/0000-0003-1739-9452
Sara Garcia-Ratés https://orcid.org/0000-0002-1848-4811
Paul Morrill https://orcid.org/0000-0002-2428-0145
Sibah Hasan https://orcid.org/0000-0002-5127-084X
Nikisha Carty https://orcid.org/0000-0002-0824-3897
Silvia Bison https://orcid.org/0000-0002-7727-8532
Laura Piccoli https://orcid.org/0000-0001-7396-4909
Renzo Carletti https://orcid.org/0000-0003-2275-2281
Stephano Tacconi https://orcid.org/0000-0003-2705-2989
Matthew Pedercini https://orcid.org/0000-0003-3169-5469
Tim Kroecher https://orcid.org/0000-0003-0060-1407
Hubert Astner https://orcid.org/0000-0001-9941-8455

REFERENCES

1. Greenfield S, Vaux DJ. Parkinson's disease, Alzheimer's disease and motor neurone disease: identifying a common mechanism. *Neuroscience*. 2002;113:485-492.

2. Day T, Greenfield SA. Bioactivity of a peptide derived from acetylcholinesterase in hippocampal organotypic cultures. *Exp Brain Res*. 2004;155:500-508.

3. Badin AS, Morrill P, Devonshire IM, Greenfield SA. II) Physiological profiling of an endogenous peptide in the basal forebrain: age-related bioactivity and blockade with a novel modulator. *Neuropharmacology*. 2016;105:47-60.

4. Ferrati G, Brai E, Stuart S, Marino C, Greenfield SA. A multidisciplinary approach reveals an age-dependent expression of a novel bioactive peptide, already involved in neurodegeneration, in the postnatal rat forebrain. *Brain Sci*. 2018;8:132.

5. Jellinger KA. Head injury and dementia. *Curr Opin Neurol*. 2004;17:719-723.

6. Mattson MP, Duan W, Pedersen WA, Culmsee C. Neurodegenerative disorders and ischemic brain diseases. *Apoptosis*. 2001;6:69-81.

7. Smith MA, Perry G. Free radical damage, iron, and Alzheimer's disease. *J Neurol Sci*. 1995134:92-94.

8. Austad SN, Hoffman JM. Is antagonistic pleiotropy ubiquitous in aging biology? *Evol Med Public Health*. 2018;2018:287-294.

9. Williams GC. Pleiotropy, natural selection, and the evolution of senescence. *Evolution*. 1957;11(4):398. https://doi.org/10.2307/2406060

10. Greenfield SA, Day T, Mann EO, Bermudez I. A novel peptide modulates alpha7 nicotinic receptor responses: implications for a possible trophic-toxic mechanism within the brain. *J Neurochem*. 2004;90:325-331.

11. Bond CE, Zimmermann M, Greenfield SA. Upregulation of alpha7 nicotinic receptors by acetylcholinesterase C-terminal peptides. *PLoS One*. 2009;4:e4846.

12. Cottingham MG, Hollinshead MS, Vaux DJ. Amyloid fibril formation by a synthetic peptide from a region of human acetylcholinesterase that is homologous to the Alzheimer's amyloid-beta peptide. *Biochemistry*. 2002;41:13539-13547.

13. Hampel H, Mesulam MM, Cuello AC, Farlow MR, Giacobini E, Grossberg GT, et al. The cholinergic system in the pathophysiology and treatment of Alzheimer's disease. *Brain*. 2018;141:1917-1933.

14. Lehner KR, Silverman HA, Addorisio ME, Roy A, Al-Onaizi MA, Levine Y, et al. Forebrain cholinergic signaling regulates innate immune responses and inflammation. *Front Immunol*. 2019;10:585.

15. Kinney JW, Bemiller SM, Murtishaw AS, Leisgang AM, Salazar AM, Lamb BT. Inflammation as a central mechanism in Alzheimer's disease. *Alzheimers Dement (N Y)*. 2018;4:575-590.

16. Beeri R, Andres C, Lev-Lehman E, Timberg R, Huberman T, Shani M, et al. Transgenic expression of human acetylcholinesterase induces progressive cognitive deterioration in mice. *Curr Biol*. 1995;5:1063-1071.

17. Garcia-Rates S, Morrill P, Tu H, Pottiez G, Badin AS, Tormo-Garcia C, et al. I) Pharmacological profiling of a novel modulator of the alpha7 nicotinic receptor: blockade of a toxic acetylcholinesterase-derived peptide increased in Alzheimer brains. *Neuropharmacology*. 2016;105:487-499.

18. Badin AS, Eraifej J, Greenfield S. High-resolution spatio-temporal bioactivity of a novel peptide revealed by optical imaging in rat orbitofrontal cortex in vitro: possible implications for neurodegenerative diseases. *Neuropharmacology*. 2013;73:10-18.

19. Arendt T, Bruckner MK, Lange M. Bigl V. Changes in acetylcholinesterase and butyrylcholinesterase in Alzheimer's disease resemble embryonic development—a study of molecular forms. *Neurochem Int*. 1992;21:381-396.

20. Eimerl S, Schramm M. The quantity of calcium that appears to induce neuronal death. *J Neurochem*. 1994;62:1223-1226.

21. Oakley H, Cole SL, Logan S, Maus E, Shao P, Craft J, et al. Intra-neuronal beta-amyloid aggregates, neurodegeneration, and neuron loss in transgenic mice with five familial Alzheimer's disease mutations: potential factors in amyloid plaque formation. *J Neurosci*. 2006;26:10129-10140.

22. Jawhar S, Trawicka A, Jenneckens C, Bayer TA, Wirths O. Motor deficits, neuron loss, and reduced anxiety coinciding with axonal degeneration and intraneuronal Abeta aggregation in the 5XFAD mouse model of Alzheimer's disease. *Neurobiol Aging*. 2012;33:196 e29-40.

23. Creighton SD, Mendell AL, Palmer D, Kalisch BE, MacLusky NJ, Prado VF, et al. Dissociable cognitive impairments in two strains of transgenic Alzheimer's disease mice revealed by a battery of object-based tests. *Sci Rep*. 2019;9:57.

24. Bhattacharya S, Haertel C, Maelicke A, Montag D. Galantamine slows down plaque formation and behavioral decline in the 5XFAD mouse model of Alzheimer's Disease. *PLoS ONE*. 2014;9(2):e89454. https://doi.org/10.1371/journal.pone.0089454

25. Sadleir KR, Eimer WA, Cole SL, Vassar R. Abeta reduction in BACE1 heterozygous null 5XFAD mice is associated with transgenic APP level. *Mol Neurodegener*. 2015;10:1.

26. Bundy JL, Vied C, Badger C, Nowakowski RS. Sex-biased hippocampal pathology in the 5XFAD mouse model of Alzheimer's disease: a multi-omic analysis. *J Comp Neurol*. 2019;527:462-475.

27. Texido L, Ros E, Martin-Satue M, Lopez S, Aleu J, Marsal J, et al. Effect of galantamine on the human alpha7 neuronal nicotinic acetylcholine receptor, the Torpedo nicotinic acetylcholine receptor and spontaneous cholinergic synaptic activity. *Br J Pharmacol*. 2005;145:672-678.

28. Brai E, Simon F, Cogoni A, Greenfield SA. Modulatory effects of a novel cyclized peptide in reducing the expression of markers linked to Alzheimer's disease. *Front Neurosci*. 2018;12:362.

29. Pietrowsky R, Strüben C, Mölle M, Fehm HL, Born J. Brain potential changes after intranasal vs. intravenous administration of vasopressin: evidence for a direct nose-brain pathway for peptide effects in humans. *Biol Psychiatry*. 1996;39(5):332–340. https://doi.org/10.1016/0006-3223(95)00180-8

30. Antunes M, Biala G. The novel object recognition memory: neurobiology, test procedure, and its modifications. *Cogn Process*. 2012;13:93-110.

31. Braak H, Braak E. Neuropathological stageing of Alzheimer-related changes. *Acta Neuropathol*. 1991;82:239-259.

32. Bielefeld-Sevigny M. AlphaLISA immunoassay platform— the "no-wash" high-throughput alternative to ELISA. *ASSAY Drug Dev Technol*. 2009;7(1):90–92. https://doi.org/10.1089/adt.2009.9996

33. Zenaro E, Piacentino G, Constantin G. The blood-brain barrier in Alzheimer's disease. *Neurobiol Dis*. 2017;107:41-56.

34. Montagne A, Zhao Z, Zlokovic BV. Alzheimer's disease: a matter of blood-brain barrier dysfunction? *J Exp Med*. 2017;214:3151-3169.

35. O'Leary TP, Mantolino HM, Stover KR, Brown RE. Age-related deterioration of motor function in male and female 5xFAD mice from 3 to 16 months of age. *Genes Brain Behav*. 2020;19:e12538.

36. Webster SJ, Bachstetter AD, Nelson PT, Schmitt FA, Van Eldik LJ. Using mice to model Alzheimer's dementia: an overview of the clinical disease and the preclinical behavioral changes in 10 mouse models. *Front Genet*. 2014;5:88.

37. Henderson Z, Greenfield SA. Ultrastructural localization of acetylcholinesterase in substantia nigra: a comparison between rat and guinea pig. *J Comp Neurol*. 1984;230:278-286.

38. Jean L, Thomas B, Tahiri-Alaoui A, Shaw M, Vaux DJ. Heterologous amyloid seeding: revisiting the role of acetylcholinesterase in Alzheimer's disease. *PLoS One*. 2007;2:e652.

39. Garcia-Ayllon MS, Small DH, Avila J, Saez-Valero J. Revisiting the role of acetylcholinesterase in Alzheimer's disease: cross-Talk with P-tau and beta-Amyloid. *Front Mol Neurosci*. 2011;4:22.

40. Lauretti E, Dincer O, Praticò D. Glycogen synthase kinase-3 signaling in Alzheimer's disease. *Biochimica et Biophys Acta Mol Cell Res.* 2020;1867(5):118664. https://doi.org/10.1016/j.bbamcr.2020.118664

41. Garrido C, Galluzzi L, Brunet M, Puig PE, Didelot C, Kroemer G. Mechanisms of cytochrome c release from mitochondria. *Cell Death Differ.* 2006;13:1423-1433.

42. Day T, Greenfield SA. A peptide derived from acetylcholinesterase induces neuronal cell death: characterisation of possible mechanisms. *Exp Brain Res.* 2003;153:334-342.

SUPPORTING INFORMATION

Additional supporting information may be found in the online version of the article at the publisher's website.